JOURNAL OF SOLID STATE CHEMISTRY 11, 1–9 (1974)

# Synthesis of New High-Pressure Columbite Phases Containing Pentavalent Vanadium

M. GONDRAND, A. COLLOMB, J. C. JOUBERT AND R. D. SHANNON*

*Laboratoire des Rayons X, C.N.R.S., B.P. No. 166, Centre de Tri, 38042 Grenoble Cedex, France*

Received August 23, 1973

A series of $MV_2O_6$ compounds with M = Ni, Mg, Co, Zn, Mn, and Cd having the orthorhombic columbite-type structure has been prepared at pressures of 50–80 kbar and temperatures of 800–1200°C. $CuV_2O_6$II was found to have a monoclinic distortion with probable space group $P2_{1/c}$ and $a = 4.824(1)$, $b = 13.483(2)$, $c = 5.652(1)$ Å and $\beta = 91.02(2)$. The transition from the brannerite to columbite-type structures involves an increase of $V^{5+}$ coordination from $5 + 1 \rightarrow 6$, a change in oxygen packing from cubic close-packed to hexagonal close-packed, a retention of part of the structure of the $VO_6$ sheets and a collapse of the $MO_6$ rutile-like chanins into $\alpha PbO_2$ chains.

The relative stabilities of the trirutile, columbite, and $PbSb_2O_6$ structures are discussed in terms of electrostatic repulsion forces, polarization, and covalency. It is concluded that minimization of cation–cation repulsion for $d^{10}$ ions cannot be responsible for the stability of the trirutile structure, since the $d^{10}$ ions $As^{5+}$ and $Sb^{5+}$ are frequently found in the $PbSb_2O_6$ structure in which each $Sb^{5+}$ or $As^{5+}$ ion has 3 $Sb^{5+}$ or $As^{5+}$ neighbors.

In plots of $r_M^3$ vs unit cell volumes for $MV_2O_6$ and $MNb_2O_6$ compounds, the volume of the Mg-containing compound always lies above the line connecting the other compositions. This deviation is attributed to the relatively greater covalence and consequent shortening of M–O bonds where M = Ni, Co, Zn, Mn, and Cd.

## Introduction

In ternary oxides $M_xV_yO_z$ pentavalent vanadium is 4-, 5- or 6-coordinated. Thus, by analogy with other compounds containing cations showing variable coordination, i.e., $B^{3+}$, $Si^{4+}$, $Ge^{4+}$ (*1*), and $Mo^{6+}$ (*2*), we anticipate that in certain instances high pressure will increase the coordination of $V^{5+}$. Indeed, this has already been demonstrated in the cases of $CrVO_4$ (*3*), $FeVO_4$ (*3*, *4*) and $Hg_2V_2O_7$ (*5*). In normal-pressure $CrVO_4$ and $FeVO_4$ vanadium is tetrahedrally coordinated; application of a pressure of 60 kbar produces structures containing octahedral $V^{5+}$–$CrVO_4$ with a disordered rutile-type structure and $FeVO_4$ with a wolframite-type structure. The structure of the normal-pressure phase of $Hg_2V_2O_7$ recently determined by Quarton et al. (*6*) contains 5-coordinated $V^{5+}$; at pressures of 30–65 kbar it transforms to the pyrochlore structure with octahedral $V^{5+}$ (*5*).

At normal pressures, the phases $MV_2O_6$ with M = Co, Zn, Mg, Cd, and Hg (*7–10*) have the brannerite ($ThTi_2O_6$) structure (*11*). $CuV_2O_6$ has been reported to exhibit two structures at normal pressures, both closely related to the brannerite structure (*12*, *13*). In the brannerite and brannerite-related structures, the $M^{2+}$ ions are octahedrally coordinated and the $V^{5+}$ ions have $5 + 1$ coordination. The vanadium ions have occasionally been described as 5-coordinated because the sixth oxygen atom is only weakly bonded (*7*, *14*) at distances of 2.4–2.8 Å. In this paper we report syntheses of the high-pressure phases $MV_2O_6$ where M = Ni, Co, Cu, Zn, Mg, Mn, and Cd with

* On leave of absence from Central Research Department, E.I. Du Pont de Nemours, Wilmington, Delaware.

Copyright © 1974 by Academic Press, Inc.
All rights of reproduction in any form reserved.
Printed in Great Britain

TABLE I

EXPERIMENTAL CONDITIONS FOR PREPARATION OF $M^{2+}V_2^{5+}O_6$ COMPOUNDS WITH COLUMBITE STRUCTURE

| $M^{2+}$ | Starting material | Pressure (kbar) | Temperature (°C) | Time (*h*) | Product | Crystals (*) | Impurities (+) |
|---|---|---|---|---|---|---|---|
| Ni | + NiO, $V_2O_5$ | 50 | 900 | 1 | $NiV_2O_6$II | | |
| Mg | + MgO, $V_2O_5$ | 50 | 1000 | 1 | $MgV_2O_6$II | * | + |
| | | 50 | 1150 | 1 | | | + |
| Cu | + CuO, $V_2O_5$ | 30 | 750 | 1 | $CuV_2O_6$I | * | |
| | | 50 | 1000 | 1 | $CuV_2O_6$I + II | * | |
| | | 50 | 900 | 1 | $CuV_2O_6$II | * | |
| Co | + CoO, $V_2O_5$ | 50 | 830 | 1 | $CoV_2O_6$II | | |
| | | 80 | 900 | 1 | $CoV_2O_6$II | | |
| Zn | + ZnO, $V_2O_5$ | 50 | 1150 | 1 | $ZnV_2O_6$II | * | |
| | | 80 | 1200 | 1 | $ZnV_2O_6$II | | + |
| | + $ZnCl_2$, $2KVO_3$ | 40 | 900 | 1 | $ZnV_2O_6$II | * | + |
| | | 50 | 900 | 3 | $ZnV_2O_6$II | | |
| | | 45 | 1030 | 1 | $ZnV_2O_6$II | * | |
| Mn | + MnO, $V_2O_5$ | 50 | 900 | 1 | ? | * | + |
| | | 80 | 1000 | 1 | ? | | + |
| | | 65 | 800 | 1 | ? | | MnO |
| | $MnV_2O_6$I | 65 | 800 | 1 | $MnV_2O_6$II | | |
| Cd | + CdO, $V_2O_5$ | 50 | 700 | 1 | $CdV_2O_6$II | | CdO |
| | | 50 | 1000 | 1 | $CdV_2O_6$II | | + |
| Ca | + CaO, $V_2O_5$ | 40 | 800 | 1 | ? | * | + |
| | | 80 | 800 | 1 | ? | * | + |

the columbite-type structure.[1] This series of brannerite–columbite transitions involves an increase in $V^{5+}$ coordination and a rearrangement of octahedra similar to the rutile → $\alpha PbO_2$ transition.

## Experimental

The starting materials were reagent grade oxides for the vanadates containing Ni, Mg, Cu, Co, Zn, Cd and Ca. The oxides were thoroughly mixed, placed in a Pt capsule, heated in a belt-type apparatus at various pressures and temperatures for 1 hr, and quenched rapidly (see Table I). The details of the technique are published elsewhere (*15*, *16*). The starting material for manganese vanadate was prereacted $MnV_2O_6$ having the brannerite structure. Crystals of $ZnV_2O_6$ II were prepared by an exchange reaction of the type:

$$ZnCl_2 \cdot xH_2O + 2KVO_3 \rightarrow ZnV_2O_6 + 2KCl + xH_2O\cdot$$

The starting materials were placed in a Pt capsule, pressed at high temperature and quenched.

Crystals of $ZnV_2O_6$ II, $MgV_2O_6$ II and $CuV_2O_6$ II,[2] having an average dimension of 0.1 mm were obtained from the mixtures of the oxides and had generally a dark color. Crystals of $ZnV_2O_6$ II obtained from the exchange reaction were transparent and lighter in color.

[1] We call the brannerite phases $MV_2O_6$I, and the columbite phases $MV_2O_6$ II.

[2] Repeated attempts to prepare the monoclinic variety of $CuV_2O_6$ reported by Lavaud and Galy (*12*) always resulted in the triclinic phase reported by Calvo and Manolescu (*13*). Until the monoclinic phase is confirmed, we call the triclinic form $CuV_2O_6$ I and the columbite form $CuV_2O_6$ II.

TABLE IIA

POWDER DIFFRACTION PATTERN OF $ZnV_2O_6$ II

| $h\,k\,l$ | $I_{obs}$ | $d_{obs}$ | $d_{cal}$ |
|---|---|---|---|
| 2 0 0 | 2 | 6.783 | 6.789 |
| 3 1 0 | 45 | 3.518 | 3.517 |
| 1 1 1 | | | 3.526 |
| 3 1 1 | 100 | 2.842 | 2.842 |
| 0 2 0 | 35 | 2.795 | 2.794 |
| 0 2 1 | 30 | 2.417 | 2.418 |
| 0 0 2 | 35 | 2.412 | 2.412 |
| 6 0 0 | 10 | 2.262 | 2.263 |
| 5 1 1 | 5 | 2.179 | 2.179 |
| 3 2 1 | 35 | 2.131 | 2.132 |
| 3 0 2 | | | 2.128 |
| 3 1 2 | 15 | 1.989 | 1.989 |
| 0 2 2 | 25 | 1.826 | 1.826 |
| 6 2 0 | 15 | 1.759 | 1.758 |
| 1 3 1 | 25 | 1.723 | 1.723 |
| 3 3 0 | | | 1.722 |
| 6 0 2 | 50 | 1.651 | 1.650 |
| 6 2 1 | | | 1.652 |
| 3 3 1 | 10 | 1.622 | 1.622 |
| 3 1 3 | 30 | 1.462 | 1.462 |
| 5 3 1 | | | 1.463 |
| 6 2 2 | 10 | 1.420 | 1.421 |
| 3 3 2 | 25 | 1.402 | 1.401 |
| 9 1 1 | 35 | 1.394 | 1.394 |
| 0 2 3 | | | 1.393 |
| 5 1 3 | 10 | 1.342 | 1.343 |
| 0 4 1 | | | 1.342 |
| 7 3 0 | | | 1.343 |
| 6 4 1 | 5 | 1.155 | 1.154 |
| 7 2 3 | 5 | 1.132 | 1.131 |

TABLE IIB

POWDER DIFFRACTION PATTERN OF $CdV_2O_6$ II

| $h\,k\,l$ | $I^a$ | $d_{obs}$ | $d_{cal}$ |
|---|---|---|---|
| 2 0 0 | M | 7.16 | 7.06 |
| 3 1 0 | M | 3.63 | 3.63 |
| 1 1 1 | St | 3.62 | 3.605 |
| 4 0 0 | W | 3.54 | 3.538 |
| 3 1 1 | V. St. | 2.932 | 2.925 |
| 0 2 0 | M | 2.847 | 2.849 |
| 2 2 0 | W | 2.644 | 2.643 |
| 0 2 1 | M | 2.467 | 2.468 |
| 0 0 2 | | | 2.466 |
| 6 0 0 | W | 2.36 | 2.358 |
| 2 2 1 | W | 2.33 | 2.330 |
| 2 0 2 | | | 2.329 |
| 4 2 0 | W | 2.215 | 2.219 |
| 3 2 1 | M | 2.183 | 2.186 |
| 3 0 2 | | | 2.185 |
| 3 1 2 | W | 2.037 | 2.040 |
| 4 2 1 | W | 2.02 | 2.024 |
| 4 0 2 | | | 2.024 |
| 0 2 2 | St | 1.865 | 1.865 |
| 6 2 0 | M | 1.818 | 1.817 |
| 2 2 2 | W | 1.804 | 1.803 |

[a] W = weak, M = medium, S = strong, V. St. = very strong.

X-ray powder diffraction patterns of $NiV_2O_6$ II, $MgV_2O_6$ II, $CoV_2O_6$ II, and $CdV_2O_6$ II were taken using a CGR-Guinier camera with KCl as an internal standard. The "$d$" values were calculated using $\lambda(FeK\alpha) = 1.9373$ Å and $a(KCl) = 6.293$ Å. Powder diffraction patterns of $ZnV_2O_6$ II and $CuV_2O_6$ II were taken using a Hägg–Guinier camera with a KCl internal standard and "$d$" values calculated using $\lambda(CuK\alpha_1) = 1.54051$ Å. The diffraction patterns of $ZnV_2O_6$ II, $CdV_2O_6$ II and $CuV_2O_6$ II and cell dimensions of the $MV_2O_6$ columbite phases are shown in Tables II and III, respectively. Superstructure lines were evident in all patterns except those of $MnV_2O_6$; Thus, $MnV_2O_6$ apparently has the disordered $\alpha$-$PbO_2$ structure. It is surprising that a compound containing two ions so different in size and charge as $Mn^{2+}$ and $V^{5+}$ can disorder. This disorder would be more consistent with a change of oxidation state such as $Mn^{3+}V^{4+}V^{5+}O_6$, but no evidence confirming or rejecting such a possibility was obtained in this study. As anticipated from other studies of isotypic series of oxides containing the Jahn–Teller ion $Cu^{2+}$, the powder patterns of $CuV_2O_6$ II indicated a splitting of most of the columbite lines. Although no single crystal of $CuV_2O_6$ could be found it was possible using the strongest reflections of a multiple crystal to ascertain the unit cell and space group. Absences of $h0l$, $l \neq 2n$; $0k0$, $k \neq 2n$; and $00l$, $l \neq 2n$

TABLE IIC

POWDER DIFFRACTION OF $CuV_2O_6II$

| $h\,k\,l$ | $I_{obs}$ | $d_{obs}$ | $d_{cal}$ |
|---|---|---|---|
| 0 2 0 | 2 | 6.732 | 6.741 |
| 0 3 1 | 75 | 3.517 | 3.517 |
| 1 1 1 | | | 3.511 |
| −1 2 1 | 2 | 3.241 | 3.244 |
| −1 3 1 | 90 | 2.857 | 2.857 |
| 1 3 1 | 100 | 2.826 | 2.827 |
| 0 0 2 | | | 2.825 |
| −1 0 2 | 40 | 2.455 | 2.457 |
| −1 1 2 | 30 | 2.417 | 2.417 |
| 1 0 2 | | | 2.419 |
| 2 0 0 | 40 | 2.411 | 2.411 |
| −1 2 2 | 10 | 2.309 | 2.308 |
| 0 6 0 | 15 | 2.246 | 2.247 |
| 2 1 1 | 5 | 2.176 | 2.175 |
| −1 5 1 | | | 2.179 |
| −1 3 2 | 20 | 2.156 | 2.155 |
| 1 3 2 | 40 | 2.129 | 2.130 |
| 2 3 0 | 35 | 2.125 | 2.125 |
| −2 3 1 | 25 | 1.999 | 1.999 |
| 2 3 1 | 25 | 1.978 | 1.978 |
| −2 0 2 | 5 | 1.849 | 1.850 |
| 2 4 1 | | | 1.844 |
| 2 5 0 | 2 | 1.797 | 1.797 |
| 1 5 2 | | | 1.800 |
| 0 6 2 | 15 | 1.758 | 1.758 |
| 2 2 2 | | | 1.755 |
| 0 3 3 | 35 | 1.737 | 1.737 |
| −1 6 2 | 35 | 1.658 | 1.658 |
| 0 4 3 | 75 | 1.644 | 1.644 |
| 2 6 0 | | | 1.644 |
| −1 3 3 | | | 1.643 |
| 1 6 2 | | | 1.646 |
| −3 2 1 | 2 | 1.514 | 1.513 |
| 3 3 0 | | | 1.513 |
| −1 7 2 | | | 1.515 |
| −3 3 1 | 25 | 1.468 | 1.468 |
| 3 3 1 | 35 | 1.456 | 1.456 |
| −2 7 1 | | | 1.458 |
| 0 8 2 | 2 | 1.446 | 1.447 |
| 0 9 1 | | | 1.448 |
| −2 6 2 | 2 | 1.427 | 1.428 |
| −2 3 3 | 10 | 1.421 | 1.420 |
| 0 0 4 | 10 | 1.413 | 1.412 |
| 2 6 2 | | | 1.413 |
| −3 4 1 | | | 1.410 |
| 2 3 3 | 30 | 1.398 | 1.398 |
| 3 4 1 | | | 1.400 |
| −3 1 2 | | | 1.400 |
| −1 6 3 | 15 | 1.388 | 1.388 |
| −1 9 1 | | | 1.388 |
| −1 8 2 | | | 1.389 |
| 3 0 2 | 30 | 1.386 | 1.386 |
| 1 9 1 | | | 1.385 |
| 0 10 0 | 5 | 1.348 | 1.348 |
| 0 3 4 | | | 1.347 |

TABLE IIC—*continued*

TABLE III

CELL DIMENSIONS OF VANADATE COLUMBITE-TYPE PHASES

| Compound | $[r_M]^{3a}$ | $a$ Å | $b$ Å | $c$ Å | $\beta°$ | $\frac{V}{4}$, Å$^3$ | $\frac{V_B - V_C}{V_B}$, %[b] |
|---|---|---|---|---|---|---|---|
| $NiV_2O_6II$ | 0.33 | 13.338 ± 5 | 5.544 ± 2 | 4.845 ± 2 | | 89.6 | |
| $MgV_2O_6II$ | 0.37 | 13.56 ± 3 | 5.571 ± 7 | 4.860 ± 6 | | 91.8 | 10.0 |
| $CoV_2O_6II$ | 0.41 | 13.501 ± 9 | 5.556 ± 3 | 4.825 ± 3 | | 90.5 | 7.2 |
| $ZnV_2O_6II$ | 0.42 | 13.579 ± 2 | 5.589 ± 1 | 4.824 ± 1 | | 91.5 | 8.2 |
| $MnV_2O_6II$ | 0.57 | 13.75 ± 1 | 5.597 ± 5 | 4.874 ± 3[c] | | 93.8 | 6.2 |
| $CdV_2O_6II$ | 0.86 | 14.16 ± 1 | 5.704 ± 5 | 4.936 ± 3 | | 99.7 | 7.7 |
| $CuV_2O_6II$ | 0.39 | 4.824 ± 1 | 13.483 ± 2 | 5.652 ± 1 | 91.02 ± 2 | 91.9 | 7.5 |

[a] $r_M$ = effective ionic radius of $M^{2+}$.

[b] $V_B$ = unit cell volume of brannerite phase; $V_C$ = unit cell volume of columbite phase.

[c] This is a hypothetical columbite cell; the smaller $\alpha PbO_2$-type cell is: $a = 4.583$; $b = 5.597$; $c = 4.874$ Å.

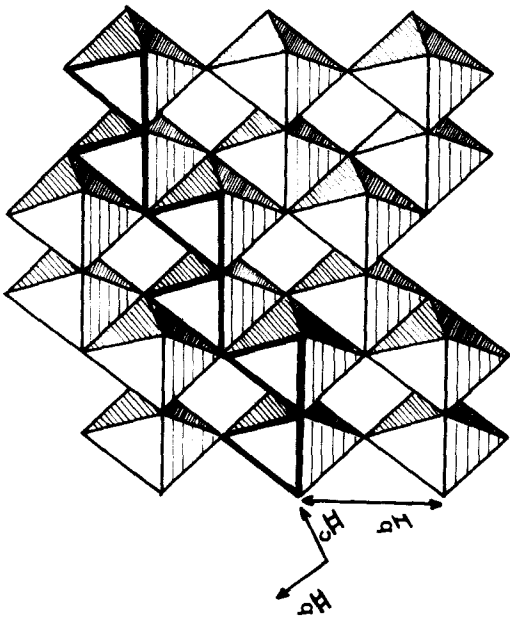

FIG. 1. A sheet of $VO_6$ octahedra in the brannerite structure (taken from Ref. 11). The octahedra formed by heavy lines are linked as in columbite (see Fig. 3b for comparison).

indicated space group $P2_{1/c}$ and the following unit cell:

$$a = 4.824 \pm 1 \text{ Å} \quad b = 13.483 \pm 2$$
$$c = 5.652 \pm 1 \quad \beta = 91.02 \pm 2.$$

The relationship between this cell and the orthorhombic columbite cell is:

$$a_{mon} = c_{ortho}$$
$$b_{mon} = a_{ortho}$$
$$c_{mon} = b_{ortho}.$$

The increase in density of the $CuV_2O_6$ columbite phase over the triclinic room pressure form is 7.5%.

## Discussion

The brannerite structure is characterized by a distorted cubic close-packed oxygen network.[3] In the brannerite-type phases, $MV_2O_6$, the $M^{2+}$ ions are octahedrally coordinated and the $V^{5+}$ ions have an irregular octahedral coordination. The $VO_6$ octahedra form infinite zigzag sheets of edge-shared octahedra parallel to the (100) planes (*11*). In Fig. 1 we show a perspective view of the $VO_6$ octahedra in the brannerite structure. Each octahedron shares an edge with 3 other octahedra. In addition we have indicated with heavy lines a columbite-type chain of octahedra which we believe is retained during the transition. Between the $VO_6$ sheets the $MO_6$ octahedra form infinite rutile-like chains running along the *b*-axis. Unlike rutile, however, these chains are not linked to each other; they provide a rather open structure between the $VO_6$ sheets. The brannerite → columbite transition thus involves a change from a cubic close-packed to a hexagonal close-packed oxygen network, a retention of part of the structure of the $VO_6$ sheets, and a collapse of the $MO_6$ rutile-like chains into $\alpha PbO_2$ chains. The volume changes resulting from the brannerite-columbite transitions are of the order of 8% (see Table III).

The stability field of the II–V columbite structure is outlined in Fig. 1. As in the case of several other structures, e.g., rutile (*17*), perovskite (*18*), and pyrochlore (*19*), the use of pressure considerably extends the stability field of the columbite structure. Several runs were made in an effort to extend the columbite

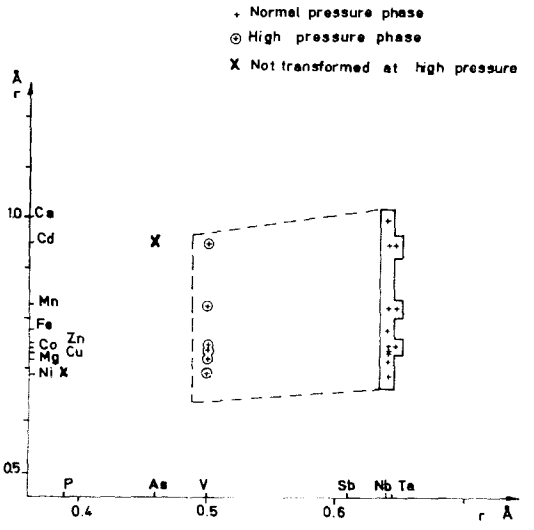


FIG. 2. Stability field of $M^{2+}M_2^{5+}O_6$ compositions having the columbite structure.

[3] This structural feature of brannerite was kindly pointed out to us by Dr. Sten Andersson.

stability field to arsenates and phosphates. The compound $CdAs_2O_6$ was heated to 900°C and 80 kbar, and quenched; however, the $PbSb_2O_6$ structure remained unchanged. We subjected $NiP_2O_6$ to a pressure of 80 kbar at 750°C, and 1000°C for 1 hr. Although a transition to a slightly denser (~ 2%) monoclinic form isotypic with $\alpha_2ZnP_2O_6$ (*20*) was found, no coordination change of the $P^{5+}$ occurred. Apparently, very high pressures will be necessary to produce octahedral $P^{5+}$.

In the $A^{2+}B^{5+}O_6$ stability field containing octahedral cations there are 3 structures in question: trirutile, columbite, and $PbSb_2O_6$. All three structures are characterized by hexagonal close-packed oxygen arrays and octahedral cations. Thus, the relative densities will be similar for all three. The fact that the trirutile and $PbSb_2O_6$ structures fall within the columbite stability field shows that ionic size is not the most important factor.

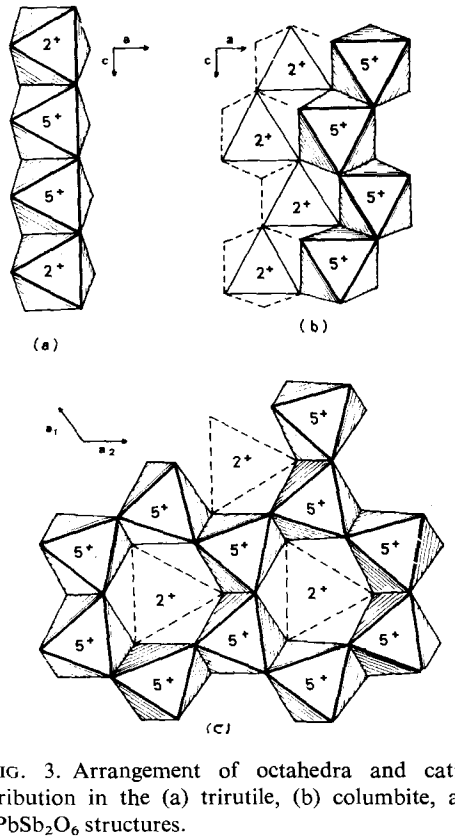


FIG. 3. Arrangement of octahedra and cation distribution in the (a) trirutile, (b) columbite, and (c) $PbSb_2O_6$ structures.

It has been previously noted by Blasse (*21*, *22*) and Goodenough and Kafalas (*23*) that structural differences between numerous compounds containing $Nb^{5+}$ and $Sb^{5+}$ arise because of differences in the electron configurations of $Nb^{5+}$ ($d^0$) and $Sb^{5+}$ ($d^{10}$). Here we note that the synthesis of the $MV_2O_6$ columbite phases strengthens the observation that $d^0$ cations ($V^{5+}$, $Nb^{5+}$, and $Ta^{5+}$) behave differently from the $d^{10}$ cations ($As^{5+}$ and $Sb^{5+}$). The differences in electronic structure lead to different degrees of electrostatic repulsion, covalency, and polarization forces (*21–23*).

We begin with an analysis of electrostatic repulsion forces in these structures. In trirutile (*24*) there exist infinite *c*-axis chains of $M^{2+}$–$Nb^{5+}$–$Nb^{5+}$–$M^{2+}$ (Fig. 3a). The columbite structure (*25*) is characterized by infinite zigzag chains of $M^{2+}$–$M^{2+}$–$M^{2+}$ and $Nb^{5+}$–$Nb^{5+}$–$Nb^{5+}$ along the *c*-axis (Fig. 3b). In the $PbSb_2O_6$ structure there are alternate layers of $PbO_6$ and $SbO_6$ octahedra (*26*). The $SbO_6$ octahedra form a hexagonal network in which each octahedron shares an edge with 3 other octahedra (see Fig. 3c). The isolated $PbO_6$ octahedra share corners with the $SbO_6$ octahedra. Blasse (*21*) analysed the structural differences between numerous compounds containing $Sb^{5+}$ and $Nb^{5+}$ and based on cation–cation repulsion considerations concluded that $Sb^{5+}$ with its $d^{10}$ electron configuration prefers structures in which each $Sb^{5+}$ ion has as few $Sb^{5+}$ neighbors as possible. In contrast $Nb^{5+}$ because of its $d^0$ configuration and its resulting ability to form $\pi$ bonds was able to enter into structures in which $Nb^{5+}$ ions can have more than one $Nb^{5+}$ neighbor.

Thus, Blasse concluded that $MSb_2O_6$ phases form the trirutile structure in which each $M^{5+}$ ion has only one neighboring $M^{5+}$ ion whereas the $MNb_2O_6$ phases have the columbite structure in which each $Nb^{5+}$ ion has 2 $Nb^{5+}$ neighbors. However, in his analysis of $M^{2+}M_2^{5+}O_6$ compounds, he neglected the $PbSb_2O_6$ structure which is formed by many arsenates and antimonates. Since, in this structure, each $Sb^{5+}$ (or $As^{5+}$) ion has three $Sb^{5+}$ ($As^{5+}$) neighbors and the repulsion effects must be very great, minimization of

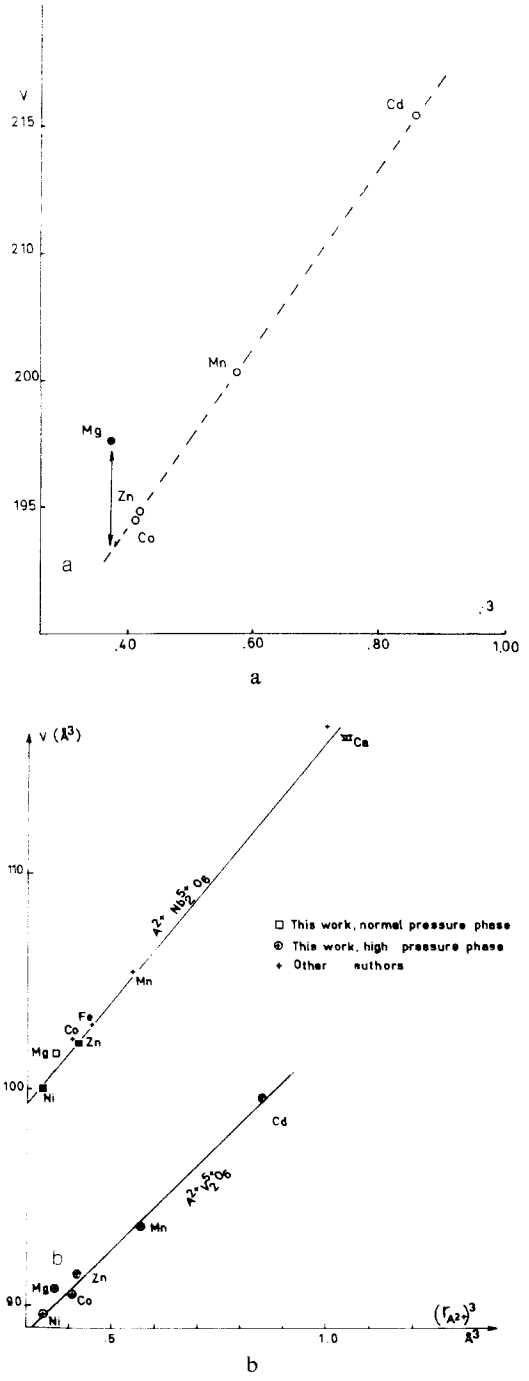


FIG. 4. Unit cell volume vs $r_M^3$ for the phases: (a) $MV_2O_6$I having the brannerite structure, and (b) $MV_2O_6$II and $MNb_2O_6$ having the columbite structure.

TABLE IV

UNIT CELL DIMENSIONS OF $NiNb_2O_6$, $MgNb_2O_6$, AND $ZnNb_2O_6$

| Compound | $a$ Å | $b$ Å | $c$ Å | V Å$^3$ |
|---|---|---|---|---|
| $NiNb_2O_6$ | 14.034(10) | 5.678(3) | 5.020(4) | 100.0 |
| $MgNb_2O_6$ | 14.187(10) | 5.702(3) | 5.030(4) | 101.7 |
| $ZnNb_2O_6$ | 14.194(7) | 5.721(2) | 5.030(3) | 102.1 |

electrostatic forces cannot be responsible for stabilization of the $Sb^{5+}$ compounds.

An analysis of covalency and polarization effects can be made by noting the environments of the oxygen atoms in the three structures. In trirutile and $PbSb_2O_6$ each oxygen is surrounded by 2 $Sb^{5+}$ and one $M^{2+}$ cations. In columbite, one oxygen atom has 3 $Nb^{5+}$ neighbors; one has 2 $Nb^{5+}$ and 1 $M^{2+}$; and one has 1 $Nb^{5+}$ and 2 $M^{2+}$ neighbors. Blasse has noted that $Sb^{5+}$ prefers structures where the anions can be strongly polarized and this is consistent with the fact that the $Sb^{5+}$ is found in both trirutile and $PbSb_2O_6$ structures and not generally in the columbite structures with the $Nb^{5+}—O^{2-}$ ($Nb^{5+}$, $Nb^{5+}$) configuration.[4]

Goodenough and Kafalas (*23*) consider that $\sigma$ bond covalency can stabilize a structure. This stabilization energy will be greater for structures containing $Sb^{5+}$ both because of the greater electronegativity of $Sb^{5+}$ (2.2) compared with $Nb^{5+}$ (1.6) and because of the tendency of $Nb^{5+}$ to lose $\sigma$ bond character by formation of $\pi$ bonds. Covalent stabilization will be strongest in structures with 90° $Sb^{5+}$–$O^{2-}$–$Sb^{5+}$ interaction because two different $Op_\sigma$ orbitals are utilized rather than one in 180° configurations. Thus, configurations

[4] However such a configuration is not impossible for $Sb^{5+}$. It has been reported in the columbite $MnSb_2O_6$ (*27*) and in $K_3Sb_5O_{14}$ (*28*). Although Brandt did not unambiguously identify $MnSb_2O_6$ as having the columbite structure, there is no doubt about the environment of the oxygen atoms in $K_3Sb_5O_{14}$.

with $Sb^{5+}$ on the same side of the anion are preferred and the hypothetical configuration

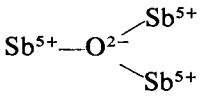

for antimonate columbites is not as energetically favorable.

In Figs. 4a and 4b the unit cell volumes of the brannerite-type vanadates and columbite-type niobates[5] and vanadates are plotted as a function of the cube of the radius of the $M^{2+}$ cation ($r_M$). It is apparent that $MgNb_2O_6$ and $MgV_2O_6$ deviate considerably from the curves. In all three plots the line connecting the volumes of the compounds containing the more electronegative elements Ni, Co, Zn, Mn, and Cd is lower than a hypothetical line connecting the less electronegative Mg- and Ca-containing compounds.[6] We believe these deviations are real and can be explained on the basis of the relative differences in degree of covalence of Mg–O bonds and M–O bonds where M = Ni, Co, Cu, Zn, Mn, and Cd. We attribute the reduced volume of oxides containing Ni, Co, Zn, Mn, and Cd to the increased covalence of the M–O bond when O is also coordinated to an electronegative cation such as $V^{5+}$. A similar covalent shortening of bond distances was found in an analysis of tetrahedral $V^{5+}$–O and $Mo^{6+}$–O distances (*34*, *35*).

## Acknowledgments

We would like to thank M. Perroux for assistance in carrying out the high-pressure experiments and Drs. A. W. Sleight and J. F. Whitney of the Central Research Department, E. I. du Pont de Nemours, for obtaining the Hägg–Guinier photographs. We would also like to thank Drs. J. A. Kafalas and J. B. Goodenough for pointing out the importance of covalent bonding energy in antimonates.

[5] The unit cell dimensions used for the niobate plot were those of Cummings and Simonsen (*29*) for $CaNb_2O_6$, Senegas and Galy (*30*) for $NiNb_2O_6$, Schroecke (*31*) for $FeNb_2O_6$, Weitzel and Klein (*32*) for $CoNb_2O_6$, and Brandt (*27*) for $MnNb_2O_6$ and $ZnNb_2O_6$. In order to confirm the relative positions of $MgNb_2O_6$, $NiNb_2O_6$ and $ZnZb_2O_6$ we redetermined the cell dimensions of these three compounds (see Table IV).

[6] It must be remembered that the radii used in these plots are the radii which were derived from the MO compounds and which give a linear plot for *these* oxides (*33*).

## References

1. J. C. JOUBERT AND J. CHENAVAS, New phases from high pressure, *in* "Treatise on Solid State Chemistry," Vol. IV (N. B. Hannay, (Ed.), 1973.
2. A. W. SLEIGHT AND B. L. CHAMBERLAND, *Inorg. Chem.* **7**, 1672 (1968).
3. A. P. YOUNG AND C. M. SCHWARTZ, *Acta Cryst.* **15**, 1305 (1962).
4. F. LAVES, A. P. YOUNG, AND C. M. SCHWARTZ, *Acta Cryst.* **17**, 1476 (1964).
5. A. W. SLEIGHT, *Mater. Res. Bull.* **7**, 827 (1972).
6. M. QUARTON, J. ANGENAULT, AND A. RIMSKY, *Acta Cryst.* **B29**, 567 (1973).
7. J. ANGENAULT, *Rev. Chim. Minérale* **7**, 651 (1970).
8. J. C. BOULOUX AND J. GALY, *Bull. Soc. Chim. France* 736 (1969).
9. H. NG AND C. CALVO, *Canad. J. Chem.* **50**, 3619 (1972).
10. C. CALVO, personal communication.
11. R. RUH AND A. D. WADSLEY, *Acta Cryst.* **21**, 974 (1966).
12. D. LAVAUD AND J. GALY, *Bull. Soc. Franc. Mineral. Crist.* **95**, 134 (1972).
13. C. CALVO AND D. MANOLESCU, *Acta Cryst.* **B29**, 1743 (1973).
14. J. ANGENAULT AND A. RIMSKY, *Compt. Rend. Acad. Sci. Paris* **267C**, 227 (1968).
15. J. CHENAVAS, These d'Etat, Grenoble (1973).
16. J. CHENAVAS, J. C. JOUBERT, J. J. CAPPONI, AND M. MAREZIO, *J. Solid State Chem.* **6**, 1 (1973).
17. R. D. SHANNON AND C. T. PREWITT, Crystal Chemistry of High Pressure Phases, Mineralogical Soc. Amer. Mtg., Mexico City, Mexico, Nov. 13, 1968.
18. R. D. SHANNON, *Inorg. Chem.* **6**, 1474 (1967).
19. R. D. SHANNON AND A. W. SLEIGHT, *Inorg. Chem.* **7**, 1649 (1968).
20. M. BEUCHER AND J. C. GRENIER, *Mater. Res. Bull.* **3**, 643 (1968).
21. G. BLASSE, *J. Inorg. Nucl. Chem.* **26**, 1191 (1964).
22. G. BLASSE, *J. Inorg. Nucl. Chem.* **27**, 993 (1965).
23. J. GOODENOUGH AND J. KAFALAS, *J. Solid State Chem.* **6**, 493 (1973).
24. A. BYSTRÖM, B. HOK AND, B. MASON, *Arkiv Kemi, Miner. Geol.* **15B**, 4 (1941).
25. J. H. STURDIVANT, *Z. Krist.* **75**, 89 (1930).
26. A. MAGNÈLI, *Arkiv Kemi, Miner. Geol.* **15B**, 3 (1941).
27. K. BRANDT, *Arkiv Kemi, Miner. Geol.* **17A**, 15 (1943).

*28.* B. AURIVILLIUS, *Arkiv Kemi* **25**, 505 (1964).

*29.* J. P. CUMMINGS AND S. H. SIMONSEN, *Amer. Mineralogist* **555**, 90 (1970).

*30.* J. SENEGAS AND J. GALY, *J. Solid State Chem.* **5**, 481 (1972).

*31.* H. SCHROECKE, *Beitr. Mineral. Petrog.* **8**, 92 (1961).

*32.* H. WEITZEL AND S. KLEIN, *Solid State Commun.* **12**, 113 (1973).

*33.* R. D. SHANNON AND C. T. PREWITT, *J. Inorg. Nucl. Chem.* **32**, 1427 (1970).

*34.* R. D. SHANNON, *Chemical Commun.* **881** (1971).

*35.* R. D. SHANNON AND C. CALVO, *J. Solid State Chem.* **6**, 538 (1973).